Toxicology Letters 325 (2020) 14–24

Contents lists available at ScienceDirect

Toxicology Letters

journal homepage: www.elsevier.com/locate/toxlet

Soluble silver ions from silver nanoparticles induce a polarised secretion of interleukin-8 in differentiated Caco-2 cells

Madeleine Polet[a], Laurie Laloux[a], Sébastien Cambier[b], Johanna Ziebel[b], Arno C. Gutleb[b], Yves-Jacques Schneider[a,*]

[a] Louvain Institute of Biomolecular Science and Technology (LIBST), Université catholique de Louvain (UCLouvain), Louvain-la-Neuve, Belgium
[b] Environmental Research and Innovation (ERIN) Department, Luxembourg Institute of Science and Technology (LIST), Esch/Alzette, Luxembourg

ARTICLE INFO

Keywords:
Silver nanoparticles
In vitro
Intestinal inflammation
Interleukin-8
Caco-2 cells

ABSTRACT

Because of their antimicrobial properties, silver nanoparticles are increasingly incorporated in food-related and hygiene products, which thereby could lead to their ingestion. Although their cytotoxicity mediated by oxidative stress has been largely studied, their effects on inflammation remain controversial. Moreover, the involvement of silver ions (originating from Ag0 oxidation) in their mode of action is still unclear. In this context, the present study aims at assessing the impact of silver nanoparticles on the secretion of the pro-inflammatory chemokine interleukin-8 by Caco-2 cells forming an *in vitro* model of the intestinal mucosal barrier. Silver nanoparticles induced a vectorized secretion of interleukin-8 towards the apical compartment, which is found in the medium 21 h after the incubation. This secretion seems mediated by Nrf2 signalling pathway that orchestrates cellular defense against oxidative stress. The soluble silver fraction of silver nanoparticles suspensions led to a similar amount of secreted interleukin-8 than silver nanoparticles, suggesting an involvement of silver ions in this interleukin-8 secretion.

1. Introduction

With the advances of nanotechnology, manufactured nanoparticles came on the market with promises of improved optical, catalytical, electronical or antimicrobial properties (Vigneshwaran et al., 2007; El-Nour et al., 2010; León-Silva et al., 2016; Syafiuddin et al., 2017). However, their smaller size and higher reactivity could also raise their toxicity. Among them, silver nanoparticles (AgNPs) are increasingly used in consumer products because of their antimicrobial properties (Wijnhoven et al., 2009). According to the Project of Emerging Nanotechnologies (The project on emerging nanotechnologies, 2019), AgNPs are found in the highest number of consumer products containing nanoparticles, with 50 % of the consumer products containing silver (The project on emerging nanotechnologies, 2019). In particular, "health and fitness" and "food and beverages" applications are the most represented categories for AgNPs, potentially resulting in their ingestion (Laloux et al., 2017). The presence of AgNPs has also been proven in the food additive E174 added in pastry decorations such as chocolates or silver pearls (Verleysen et al., 2015). Aside this example, AgNPs are not directly incorporated in food but can migrate into it from packaging materials, cooking instruments, cleaning sprays or storage boxes (Wijnhoven et al., 2009; Emamifar et al., 2012; Cushen et al., 2014; Echegoyen and Nerín, 2013; Hauri and Niece, 2011; Song et al., 2011; von Goetz et al., 2013). Even if the potential migrated amount remains low, the increasing use of AgNPs in consumer products could dramatically raise the consumer exposure to AgNPs. Moreover, AgNPs constitute some unauthorised food supplements whose consumption can lead to up to 0.02 mg/kg BW/day exposure (Larsen et al., 2015). After ingestion, these AgNPs will come in contact with the gut. Although the cytotoxicity of AgNPs has been largely studied, their effect on inflammation remains controversial.

Because of its major role in inflammation, we decided to focus on the production of interleukin-8 (IL-8) by intestinal epithelial cells (IECs), a chemokine involved in inflammatory processes. For this

Abbreviations: Ag^+, silver ions; AgNPs, silver nanoparticles; ARE, antioxidant response element; DLS, dynamic light scattering; DMEM, Dulbecco modified Eagle's medium; GALT, gut-associated lymphoid tissue; HBSS, Hank's balanced salt solution; HO-1, heme oxygenase-1; IECs, intestinal epithelial cells; IFN-γ, interferon-γ; IL-10, interleukin-10; IL-6, interleukin-6; IL-1β, interleukin-1β; IL-8, interleukin-8; LPS, lipopolysaccharide; MCP-1, monocyte chemoattractant protein-1; NBT, nitro blue tetrazolium; Nrf2, nuclear factor-erythroid 2-related factor; ROS, reactive oxygen species; SEM, standard error of the mean; TEM, transmission electron microscopy; TNF-α, tumor necrosis factor-α

* Corresponding author.
E-mail address: yves-jacques.schneider@uclouvain.be (Y.-J. Schneider).

https://doi.org/10.1016/j.toxlet.2020.02.004
Received 4 November 2019; Received in revised form 2 February 2020; Accepted 4 February 2020
Available online 13 February 2020
0378-4274/

purpose, Caco-2 cells were used as an *in vitro* model of the gut mucosal barrier. Although isolated from a colonic adenocarcinoma (Fogh and Trempe, 1975), they differentiate spontaneously in cells presenting characteristics similar to small intestine enterocytes such as the presence of active tight junctions and efflux pumps (Artursson, 1990; Sambuy et al., 2005; Smetanová et al., 2011). These cells are thus commonly used as a simple *in vitro* model of the small intestine in pharmaco-toxicology studies. In particular, they are the most widely used for nanomaterial translocation assessment (Braakhuis et al., 2015; Georgantzopoulou et al., 2015).

Although toxicity of AgNPs has been extensively reported in the literature, the involvement of silver ions (Ag^+) in their mode of action still remains unclear. These ions, as a subproduct of Ag0 oxidation (Reidy et al., 2013), are commonly found in AgNPs suspensions in variable proportions that can go even up to 69 % of total silver content (Beer et al., 2012), depending on the synthesis method (Beer et al., 2012), the AgNPs size (Bouwmeester et al., 2011) and concentration (Hadioui et al., 2013) or the chemical nature of their coating (van der Zande et al., 2012). Together with different chloride complexes (Behra et al., 2013), Ag^+ forms the "soluble Ag fraction" in AgNPs suspensions. Although silver salts are known to be toxic (Miura and Shinohara, 2009), only a few studies have addressed this issue. Most of the published reports concerning AgNPs have not distinguished the effect of soluble Ag from the global observed effects (Zhao and Wang, 2012). Papers addressing this issue have generally compared the effect of a silver salt such as acetate or nitrate as a source of Ag^+ (Böhmert et al., 2015; Bilberg et al., 2011; Martirosyan et al., 2016; Navarro et al., 2008; Yin et al., 2011). Only a few tests have been performed with the soluble fraction separated from AgNPs suspensions although this was recommended by Beer et al. (2012) for all studies concerning metallic nanoparticles such as silver or copper (Beer et al., 2012). In addition, AgNPs toxicity was suppressed by cysteine, which inactivates soluble Ag by complexing the ions (Zhao and Wang, 2012). Another way to assess the involvement of this soluble Ag is to separate it from the suspension, either by ultracentrifugation (Beer et al., 2012) or by filtration through a membrane with an appropriate cut-off (Zhao and Wang, 2012). Silver ions could also be separated from the rest of the suspension by ion exchange resin (Hadioui et al., 2013) although this is less used in literature.

The gut is a major immune organ, with about 60 % of the total immunoglobulin content of the human body (Salminen et al., 1998). Within this organ, the gut-associated lymphoid tissue (GALT) containing the largest pool of immune cells is found (Bourlioux et al., 2003). However, due to the presence of overwhelming potentially immune-stimulatory bacterial and food antigens, this tissue should respond adequately to stimulations. A complex regulation takes place in the gut to allow pathogens recognition while avoiding any unwanted response to the "normal" gut microflora. IECs form the first barrier encountered by luminal antigens and should respond appropriately to have a role in the regulation of immune response (Blikslager et al., 2007). For this purpose, they can secrete chemokines, cytokines and eicosanoids (Mason et al., 2008) to communicate with immune cells and to direct them selectively towards antigens. In particular, IL-8 is an important mediator for these cells, being the major secreted product of infected epithelial cells (Eckmann et al., 1995), *e.g.* Caco-2 cells (Van De Walle et al., 2010; Sergent et al., 2010). This chemokine produced among others by IECs, has the ability to attract neutrophils to guide them to the site of inflammation and it is thus commonly classified as a pro-inflammatory cytokine (Andoh et al., 2000; Rossi et al., 2013).

As the involvement of oxidative stress in the toxicity of AgNPs has been extensively proven (Völker et al., 2013; Kim and Choi, 2012; Georgantzopoulou et al., 2015; Gaillet and Rouanet, 2015; Akter et al., 2018), we have decided to evaluate whether a transcription factor *i.e.* Nuclear factor-erythroid 2-related factor (Nrf2) could be involved in this crosstalk as it orchestrates the defence against oxidative stress. Under normal conditions, Nrf2 is sequestrated by the cytosolic protein Keap1, which leads to its proteosomal degradation. Keap1 contains a series of reactive cysteine residues, acting as a sensor through reaction with electrophiles or oxidants. This modification releases Nrf2 that then translocates in the nucleus and regulates the expression of its target genes, containing an antioxidant response element (ARE) in their promoters (Kobayashi and Yamamoto, 2005). They modulate the cellular response to stress such as phase 2 detoxifying enzymes, thiol molecule generating system, reactive oxygen species (ROS) removing enzymes or stress response proteins (Kwak et al., 2004; Kobayashi and Yamamoto, 2005; Kensler et al., 2007). Among these target genes, heme oxygenase-1 (HO-1) is one of the most used to assess the activation of Nrf2 as it has been probably the best characterised ARE (Simmons et al., 2011). This enzyme, also named "heat shock protein 32", catalyzes the heme degradation, releasing free iron, bilirubin and carbon monoxide (Gozzelino et al., 2010). Moderate levels of these three molecules could exert anti-inflammatory and antioxidant properties (Ryter et al., 2006). Indeed, HO-1 seems to have a major role in the protection against acute and chronic inflammation of the gut (Zhu et al., 2011), its induction being associated with a protective response that contributes to the preservation of the gastro-intestinal tract (Zhu et al., 2011). Activation of Nrf2 (Prasad et al., 2013; van der Zande et al., 2016; Mao et al., 2018; Aueviriyavit et al., 2014; Ambrožová et al., 2017; Böhmert et al., 2015) and/or induction of HO-1 (Stępkowski et al., 2014; Bouwmeester et al., 2011; Miura and Shinohara, 2009; Xin et al., 2015; Kang et al., 2012a; Sahu et al., 2015; Ambrožová et al., 2017; Aueviriyavit et al., 2014; Fizesan et al., 2019) have been largely observed as a response to AgNPs.

In this study, we investigated if this Nrf2 cascade could play a role in the secretion of IL-8 mediated by AgNPs as IL-8 displays an ARE in its promoter (Zhang et al., 2005). This study aims at evaluating if AgNPs could modulate the secretion of IL-8 in Caco-2 cells. Moreover, we investigated the involvement of soluble Ag and Nrf2 signalling pathway in this secretion.

2. Material and methods

2.1. Cell culture and exposure

Caco-2 cells from a human colon adenocarcinoma (clone 1 from Dr. M. Rescigno, University of Milano, IT) were cultivated between p + 10 and p + 30 at 37°C under a water-saturated atmosphere with 10 % (v/v) CO_2. Caco-2 cells were grown in tissue culture flasks (Corning incorporated, Corning, NY) in Dulbecco modified Eagle's medium (DMEM) with 4.5 g/L glucose (Lonza, Basel, CH), supplemented with 10 % (v/v) fetal bovine serum (Biowest, Nuaillé, FR), 1% (v/v) non-essential amino acids 100X (Lonza), 1% (v/v) L-glutamine 200 mM in a 0.85 % NaCl solution (Lonza) and 1% (v/v) penicillin-streptomycin (Lonza). Caco-2 cells were seeded at a cell density of *ca.* 63 000 cells/cm^2 either in inserts (polycarbonate membrane with 0.4 µm pore diameter, Costar Transwell Permeable Supports, Corning incorporated) for IL-8 quantification or in culture well plates (Corning incorporated) precoated with type I collagen (Sigma-Aldrich, St. Louis, MO) for the other experiments. Cells were cultivated during 21 days upon differentiation. The day of the experiment, differentiated Caco-2 cells were exposed in Hank's balanced salt solution (HBSS) during 3 h to the different treatments, whose volume was adapted between inserts and wells taking the surface area into account.

2.2. Reagents

AgNPs < 20 nm (NM-300 K, JRC repository, Ispra, IT) were purchased from Fraunhofer institute (Schmallenberg, DE) as a dispersion in water containing 10.16 % (w/w) of silver, 4% (w/w) of polyoxyethylene glycerol trioleate and 4% (w/w) of polyoxyethylene (20) sorbitan mono-laurate (Tween 20). Stock solutions of AgNPs were prepared in milliQ water (Millipore, Burlington, MA) and diluted in

HBSS (Lonza) directly on cells to obtain a range of concentrations between 1.5 and 15 µg/mL, which was chosen to avoid any cytotoxicity (data not shown). The inflammatory cocktail was constituted of tumor necrosis factor-α (TNF-α) (50 ng/mL), interleukin-1β (IL-1β) (25 ng/mL), interferon-γ (IFN-γ) (50 ng/mL) and lipopolysaccharide (LPS) (1 µg/mL) (all coming from Sigma-Aldrich), and was developed to obtain the highest secretion by Caco-2 cells of targets of NF-κB pathway *e.g.* IL-8, IL-6, NO and PGE-2 as established by Van de Walle et al. (2010) (Van De Walle et al., 2010).

Nitric acid (70 %, highest purity), used for ICP-MS measurements, was purchased from VWR (Leuven, BE).

2.3. Cytokines measurement

Concentrations of cytokines IL-8, interleukin-6 (IL-6), monocyte chemoattractant protein-1 (MCP-1) and interleukin-10 (IL-10) were measured with specific ELISA kits (Becton Dickinson Biosciences, Franklin lakes, NJ). Nrf2 signalling cascade was inhibited by a pre-incubation of 24 h with ML-385 at 10 µM (Cayman Chemicals, Ann Arbor, MI). Cells were incubated with the different treatments during 3 h after which media were harvested. Cells were then washed once and culture medium was added for a duration called "the recovery period", varying between 0 and 21 h. Media were collected again and used to quantify different cytokines by ELISA that contained capture and detection antibodies, recombinant standard and streptavidin-horseradish peroxidase and were performed according to the manufacturer's instructions.

2.4. Separation of soluble Ag from AgNPs suspensions

Soluble silver was separated from AgNPs suspensions prepared freshly at different concentrations between 7.5 and 75 µg/mL in milliQ water using Vivaspin turbo 4 centrifugal ultrafiltration devices containing polyethersulfone membranes with a molecular weight cut off at 10 kDa (Sartorius, Göttingen, DE). Suspensions were centrifuged on ultrafiltration devices at 3220 g during 10 min. The absorbance of filtrates was measured between 350 and 750 nm by a UV–vis spectrophotometer (Thermo Fisher Scientific, Waltham, MA). As AgNPs absorb at *ca.* 410 nm, which is not the case for Ag^+, it allowed a control of the filtration process. No absorbance was observed for filtrates (Figure S1.3). Solutions were diluted 5 times in HBSS directly on cells to avoid a loss of silver due to precipitates with chlorides or phosphates. The process is illustrated in Fig. 1.

2.5. ICP-MS

Following the ultrafiltration, filtrates (containing soluble Ag) and initial suspensions (containing total silver) were acidified with 4% (v/v) nitric acid. Silver content was then quantified using an ICP-MS (7900 ICPMS, Agilent, Santa Clara, CA). The calibration curve was performed from 0.010–50 µg Ag/L with several dilutions of a multi element standard solution (Chem-lab, Zedelgem, BE, certified ISO/IEC 17025). The analytical method validity was verified every 10 measurements with 3 quality controls at 0.5, 5 and 25 µg Ag/L (Merck, Readington, NJ). The limit of quantification was 0.010 µg Ag/L. Samples were diluted so that silver concentrations were in the calibration range.

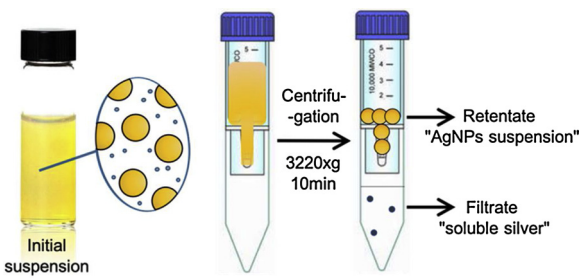

Fig. 1. Principle of the separation between AgNPs and soluble Ag.

2.6. Involvement of oxidative stress

Oxidative stress was assayed with a soluble tetrazolium salt reacting with ROS, nitro blue tetrazolium (NBT) (Sigma-Aldrich). After 3 h treatment with AgNPs, cells were washed once and incubated during 2 h with NBT diluted at 0.4 mg/mL in HBSS. Cells were rinsed and formazan salt was extracted with 1 M NaOH aqueous solution containing 50 % (v/v) DMSO (Sigma-Aldrich). Absorbance was measured at 680 nm and expressed as a percentage of untreated cells.

2.7. Gene expression study

Cells were seeded in 6 well plates and 21 days later exposed for 3 h to different treatments. Total RNA was then extracted from each well (containing *ca.* 1.10^6 cells) by a treatment with Qiazol (Qiagen, Germantown, MD) and a purification with Aurum Total RNA Mini Kit (Biorad Laboratories, Hercules, CA) according to manufacturer's protocol. RNA quality and quantity were estimated with a Nanodrop instrument (Thermo Fisher Scientific) measuring the absorbance at 230, 260 and 280 nm. Primer efficiencies were all between 1.8 and 2.0.

Total RNA integrity was assessed by gel electrophoresis on 1.5 % (w/v) agarose displaying neither contamination with genomic DNA nor degradation of RNA. 1 µg of total RNA was used for retrotranscription with the iScript cDNA Synthesis Kit (Bio-rad Laboratories) following manufacturer's instructions. cDNA coming from 3 different wells similarly treated were pooled to have enough material for the qPCR analyses and diluted to a concentration of 2 ng/µL. qPCR were performed using Takyon SYBR Green low ROX (Eurogentec, Liège, BE) on a Viia7 384well real-time PCR instrument (Thermo Fisher Scientific) according to manufacturer's instructions. A BLAST search over the human genome sequence was carried out to assess the specificity of primers. The absence of primer dimers and secondary structures was verified *in silico* with the software Amplify4 (Bill Engels, University of Wisconsin, WI).

Five reference genes were used and three of them (β-actin, HPRT1 and SDHA) were selected as the most suitable for normalisation of data using the Biogazelle algorithm in qBase+ 3.2 software (Biogazelle, Ghent, BE). Primer information are reported in Table 1 Relative expression were calculated with the ΔΔCt method taking into account multiple reference gene normalisation and specific primer PCR efficiencies (Livak and Schmittgen, 2001). Control cells were exposed to neither silver nor inflammatory cocktail and their expression level was set at 1. Efficiency and linearity for each couple of primers was estimated with a preliminary qPCR performed on a pool of all the samples for experimental validation and efficiencies estimation, which are reported in figure S1.

2.8. Cytotoxicity assay

The cytotoxicity of ML-385, a specific inhibitor of Nrf2 pathway (Singh et al., 2016), was estimated with a LDH assay (Cytotoxicity detection kit, Sigma-Aldrich). Caco-2 cells were differentiated during 21 days in 48 well-plates. Cells were incubated during 3 h in the absence or presence of ML-385 at 10 µM and medium was used for LDH activity assessment according to manufacturer's instructions. Cells treated during 0.5 h with Triton-X100 1% (v/v) HBSS (Sigma-Aldrich) were used as a positive control of lysis, set at 100 % necrosis.

2.9. Statistical analysis

All statistical analyses were performed with JMP Pro14 (SAS Institute, Cary, NC). First, normality of the data distribution and homoscedasticity were verified with respectively Shapiro-Wilk test and Levene test to determine which comparison tests should be used. When

Table 1
Primers used in the analysis of mRNA in the current study.

Targeted gene	Accession number	Amplicon size (bp)	PCR efficiency	Primer	Sequence (5'-3')	Reference
Chemokine (CXC motif) ligand 8	NM_000584.3	125	1.916	IL-8 Forward	CTGGCCGTGGCTCTCTTG	Hollebeeck et al. (2012)
				IL-8 Reverse	GTAAGGACCCATCGGAGAAGC	
Heme oxigenase-1	NM_002133	151	1.973	HMOX1 Forward	TGACACCAAGGACCAGAGCC	Wang and Seed (2003)
				HMOX1 Reverse	GGGTGGAAAGGTTTGGAGTATG	
Beta actin	NM_001101.4	119	1.908	β-actin Forward	TCCAAATATGAGATGCGTTGTT	Designed
				β-actin Reverse	AATGCTATCACCTCCCCTG	
Hypoxanthine phosphor ribosyltransferase 1	NM_000194.3	94	1.887	HPRT1 Forward	TGACACTGGCAAAACAATGCA	Klein et al. (2017)
				HPRT1 Reverse	GGTCCTTTTCACCAGCAAGCT	
Succinate dehydrogenase complex flavoprotein subunit A	NM_001294332.1	86	1.891	SDHA Forward	TGGGAACAAGAGGGCATCTG	Klein et al. (2017)
				SDHA Reverse	CCACCACTGCATCAAATTCATG	
Tyrosine 3-monooxygenase	NM_003406	94	1.922	YWHAZ Forward	ACTTTTGGTACATTGTGGCTTCAA.	Kaulmann et al. (2016)
	NM_001256799.2			YWHAZ Reverse	CCGCCAGGACAAACCAGTAT	
Glyceraldehyde-3-P	NM_001256799.2	111	1.905	GADPH Forward	ACCCACTCCTCCACCTTTGAC	Hollebeeck et al. (2012)
				GADPH Reverse	GTCCACCACCCTGTTGCTGTA	

data had a normal distribution and equal variances, ANOVA-1 was applied followed by a Dunnet's post-hoc analysis. In any other cases, Student's *t*-test were performed with type I error (α) set at 0.05 and a Bonferroni-Šidák correction of the p-values for multiple comparisons (Šidák, 1967). For gene expression analysis, the same *t*-test was applied on log-transformed data, as the reference condition (control) had no variance.

3. Results

3.1. Characterisation of the nanomaterial

The characterisation of dry particles from this batch was performed by Klein et al. (2011) (Klein et al., 2011). We also performed an additional characterisation of AgNPs in HBSS (67.5 µg/mL) by transmission electron microscopy (TEM) (Fig. 2), UV–vis spectrophotometry (Fig. 3A) and dynamic light scattering (DLS). The hydrodynamic diameter measured by DLS was 57.75 nm with a polydispersity index of 0.226. In addition, the absorbance of soluble silver fraction was measured between 350 and 750 nm as a control of the ultrafiltration process. The characteristic absorbance peak at 410 nm, found in AgNPs suspensions (Fig. 3A) is not retrieved in filtrates (Fig. 3B).

3.2. Experimental setup for IL-8 measurement

Differentiated Caco-2 cells were exposed to AgNPs during 3 h, to mimic an acute ingestion. A preliminary experiment was performed to verify if this duration was sufficient to allow the production of the inflammatory chemokine IL-8 by testing the amount of IL-8 produced after a recovery period varying between 0 and 21 h after the 3 h incubation with an inflammatory cocktail composed of LPS and three cytokines, *i.e.* TNF-α, IL-1β and IFN-γ (Fig. 4). No recovery period (0 h in Fig. 4) led to a production of 175 pg IL-8 per insert. The level of IL-8 protein increased with the duration of recovery, reaching a plateau after 15 h recovery at 4100 pg of IL-8 per insert, which suggests that IL-8 requires time to be produced and its secretion following the inflammatory stimulus is thus delayed after the incubation.

Therefore, for the other experiments presented in this study, when IL-8 protein was measured, the 3 h incubation with the different treatments was followed by a 21 h recovery period to collect the total amount of IL-8 produced due to the treatments.

3.3. Interleukin-8 secretion in response to AgNPs exposure

The ability of AgNPs to induce IL-8 secretion was then investigated on Caco-2 cells cultivated in bicameral inserts. AgNPs increased the amount of IL-8 secreted by Caco-2 cells (Fig. 5A). This effect was significant even at the concentration of 1.5 µg/mL with 780 pg and went up with the dose as 15 µg/mL led to the secretion of 1135 pg IL-8. However, this effect was not proportional: 2/3 of the effect was already observed with 1.5 µg/mL AgNPs, suggesting that the secretion of IL-8 tends to level off with increasing concentration of AgNPs.

IL-8 was differentially induced in either the apical or basolateral compartments (Fig. 5B). Indeed, all tested concentrations of AgNPs led to a significant rise of IL-8 in the apical compartment while the basolateral amount of IL-8 was affected only with 15 µg/mL AgNPs. This was not the trend observed with the inflammatory cocktail, with a higher secretion in the basolateral compartment. This situation was more representative of the physiological situation, as the basolateral compartment corresponds *in vivo* to the blood.

This effect of AgNPs on the expression of IL-8 after 3 h incubation is confirmed at the transcriptional level, as IL-8 mRNA rose with increasing concentrations of AgNPs, up to three times for the concentration of 15 µg/mL AgNPs (Fig. 6). As expected, the inflammatory cocktail dramatically increased the amount of IL-8 mRNA.

The expression levels of IL-6, MCP-1 and IL-10 were also measured

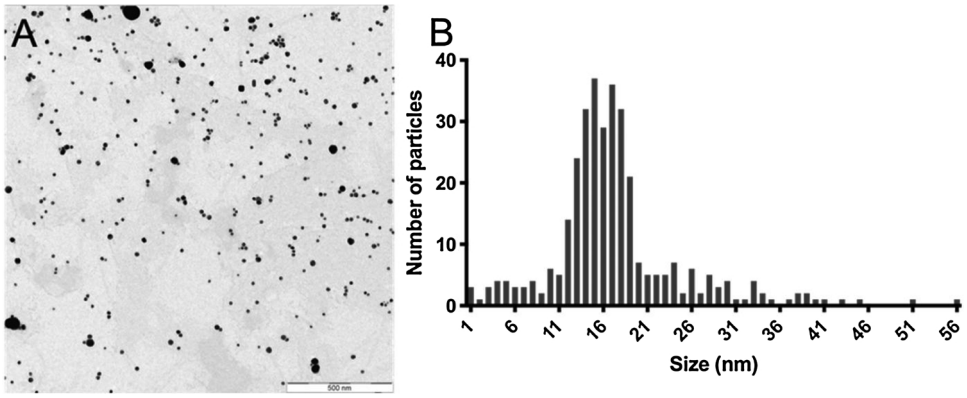

Fig. 2. TEM image (10 000x) (A) and size distribution (B) of a AgNPs suspension (NM-300 K) prepared at 67.5 µg/mL and dropped on a TEM grid. The scale bar represents 500 nm.

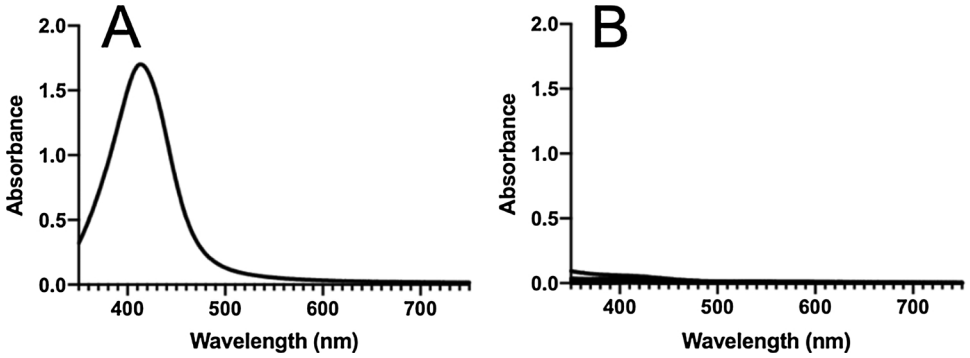

Fig. 3. Absorbance between 350 and 750 nm of (A) AgNPs suspension at 15 µg/mL in water and (B) the same suspensions after ultrafiltration on 10 kDa centrifugal devices.

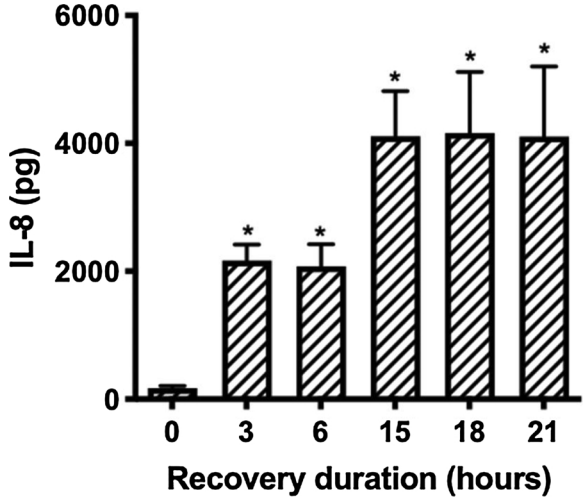

Fig. 4. Kinetics of IL-8 secretion by differentiated Caco-2 cells after 3 h exposure to the inflammatory cocktail (TNF-α, IL-1β, IFN-γ and LPS) and then allowed to recover for different durations in fresh culture medium. Samples were collected after 0, 3, 6, 15, 18 and 21 h in culture medium and IL-8 was measured by ELISA. Data are expressed as mean ± standard error of the mean (SEM) of IL-8 amount secreted per well and come from 2 independent repetitions with 4 replicates. A star indicates a significant difference with the untreated cells ("Control') ($P < 0.05$, Student's *t*-test with Bonferroni-Šidazk correction).

in these conditions but were below sensitivity of the ELISA for all the experimental conditions (except IL-6 for cells incubated with the inflammatory cocktail treatment) (data not shown).

3.4. Effect of soluble Ag ions on IL-8 secretion

AgNPs suspensions contained AgNPs but also soluble Ag deriving from the metal oxidation. A centrifugal ultrafiltration of AgNPs suspension was performed before the incubation with cells to evaluate the impact of this soluble Ag on AgNPs induction of IL-8. Initial suspensions are termed "AgNPs suspension" while the filtrates after centrifugal ultrafiltration are named "soluble Ag". No particles were able to pass through the filters (Figure S1.3). ICP-MS measurements showed that AgNPs suspensions contained up to 5% of soluble Ag, able to pass through ultrafiltration devices (Figure S2). No significant difference could be observed between AgNPs and soluble Ag contained in AgNPs suspensions on IL-8 gene transcription (Fig. 7), suggesting that the rise of IL-8 mRNA is mediated by the soluble fraction of AgNPs suspensions.

The involvement of soluble Ag was also investigated at the level of IL-8 protein, through ELISA measurements (Fig. 8): as above, differentiated Caco-2 cells were incubated with AgNPs suspensions or soluble Ag during 3 h followed by 21 h recovery period and total IL-8 was measured. In addition to these conditions, a supplementary control was performed to investigate the influence of soluble Ag on this increase of IL-8. As the majority of this soluble Ag should be in the form of ionic silver, the supplementary control consisted in a solution of silver nitrate (a soluble silver salt) containing 0.75 µg/mL Ag^+ to compare it with AgNPs suspension at 15 µg/mL.

AgNPs suspensions induce a significant secretion of IL-8 compared to control cells. Nevertheless, no significant difference was observed between AgNPs, soluble Ag and Ag^+, suggesting that the secretion of pro-inflammatory chemokine IL-8 is mediated by the soluble fraction of AgNPs suspensions, probably Ag ions as observed by a similar increase for a solution of Ag nitrate containing the same amount of Ag.

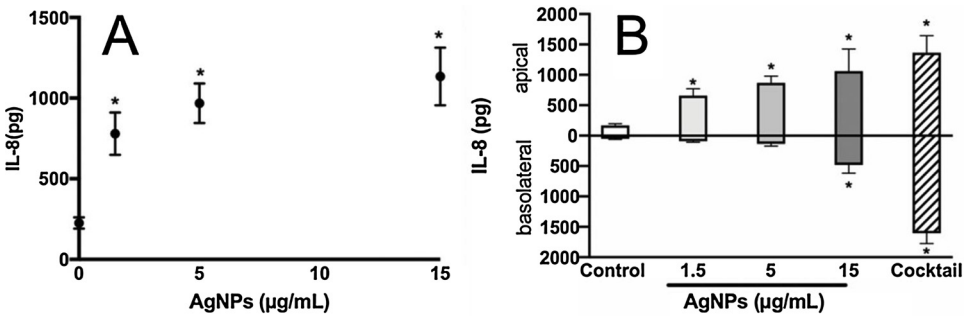

Fig. 5. IL-8 secretion by Caco-2 cells incubated with AgNPs expressed (A) as the total (sum of apical and basolateral) secretion of IL-8 after 3 h incubation with AgNPs or the inflammatory cocktail, followed by 21 h in fresh culture medium, measured by ELISA and (B) by compartment (apical in the upper part, basolateral in the lower part) in the same conditions. Data are expressed as mean ± SEM of IL-8 amount secreted per insert and come from 3 independent repetitions with 3 replicates. A star indicates a significant difference with the untreated cells ("Control") ($P < 0.05$, Student's *t*-test with Bonferroni-Šidazk correction).

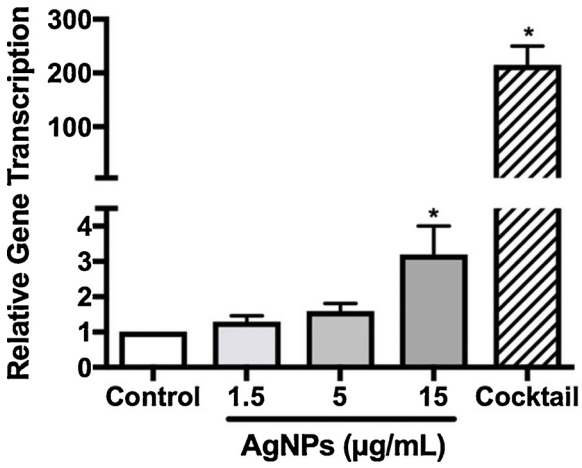

Fig. 6. Relative gene transcription of IL-8 after 3 h exposure with different concentrations of AgNPs or the inflammatory cocktail. Data are expressed as mean ± SEM and come from 4 independent repetitions with 3 technical replicates for each measure. A star indicates a significant difference with the control consisted in untreated cells ("Control") ($P < 0.05$, Student's *t*-test with Bonferroni-Šidazk correction).

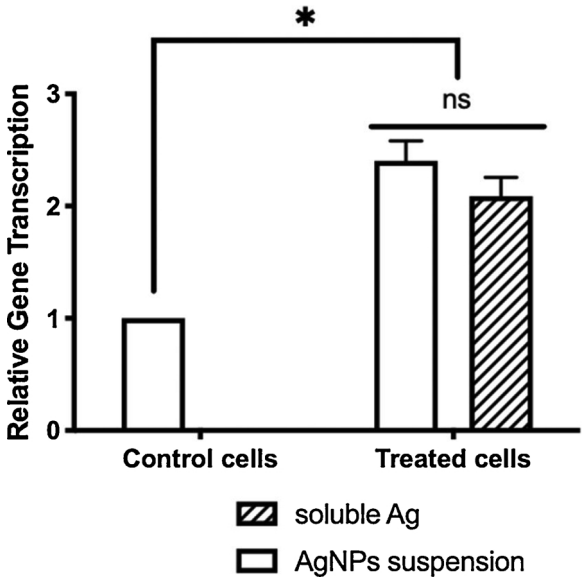

Fig. 7. Expression of IL-8 measured as relative gene transcription of IL-8 after 3 h incubation. Data are expressed as mean ± SEM and come from 4 independent biological replicates with 3 technical replicates. No significant difference was observed between soluble Ag and AgNPs although they were both different from untreated cells ("Control") ($P < 0.05$, Student's *t*-test with Bonferroni-Šidazk correction).

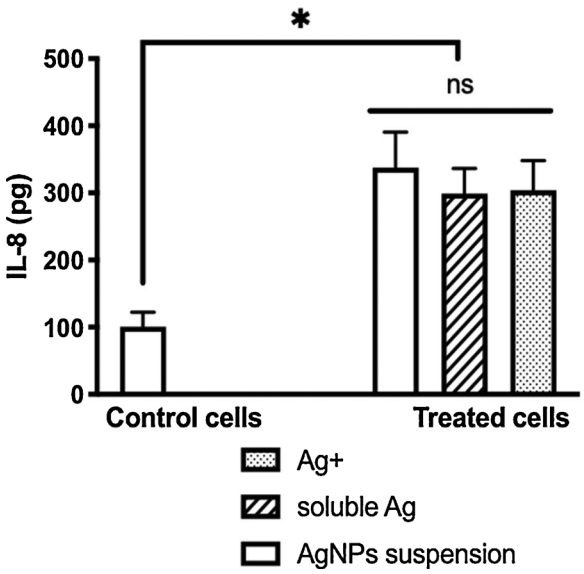

Fig. 8. Total amount of IL-8 produced after 3 h exposure to treatments followed by 21 h recovery period in fresh culture medium. Treatments consists in HBSS ("Control"), AgNPs at a concentration of 15 µg/mL filtrated (soluble Ag) or not (AgNPs suspension) with ultrafiltration devices or silver nitrate containing 0.75 µg/mL Ag. Data are expressed as mean ± SEM and come from 3 independent repetitions with 3 replicates. A star indicates a significant difference caused by treatment, while "ns" means non-significant difference ($P < 0.05$, ANOVA with Tukey-Kramer post-hoc test).

3.5. Involvement of oxidative stress and Nrf2 signalling pathway in production of IL-8

The generation of intracellular ROS was then evaluated with NBT reduction assay (Fig. 9). For this experiment, cells were incubated with AgNPs during 3 h, washed, and incubated with NBT reagent during 1 h. As NBT reacts with ROS to form blue formazan precipitates, it is correlated with the presence of intracellular ROS. AgNPs, from a concentration of 10 µg/mL, led to a significant production of blue formazan precipitate, suggesting a generation of intracellular ROS consecutive to AgNPs presence. A positive control, *i.e.* tert-butyl hydroperoxide led to the production of 200 % blue formazan precipitate compared to the untreated control (data not shown).

As the presence of superoxide anion radical is a marker of oxidative stress in cells, the involvement of Nrf2 signalling pathway, sensor of oxidative stress, was investigated. The expression of HO-1, a target enzyme of Nrf2 cascade was analysed by qPCR assay (Fig. 10). AgNPs induced the transcription of HO-1 proportionally to their concentration. Levels of HO-1 mRNA were significantly different from untreated cells from a concentration of 5 µg/mL AgNPs.

The activation of the Nrf2 transduction cascade was further analysed using ML-385, a specific inhibitor of Nrf2 (Singh et al., 2016). The

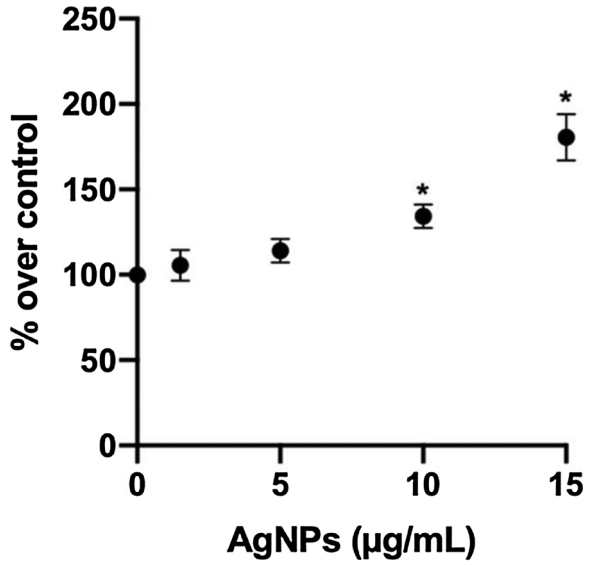

Fig. 9. Generation of intracellular ROS measured by NBT assay, in differentiated Caco-2 cells incubated with different concentrations of AgNPs. Results are expressed as a percentage of the absorbance measured after incubation of untreated cells with NBT. Data are expressed as mean ± SEM and come from 4 independent repetitions with 3 replicates. A star indicates a significant difference with the untreated cells ($P < 0.05$, Student's *t*-test with Bonferroni-Šidazk correction).

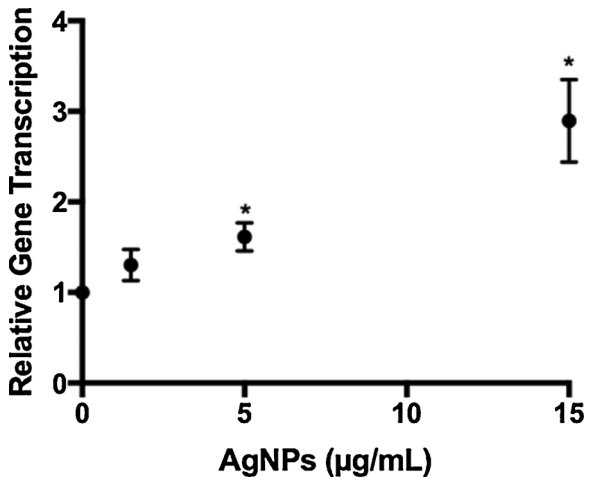

Fig. 10. Relative gene transcription of HO-1 upon 3 h exposure of differentiated Caco-2 cells with different concentrations of AgNPs. Data are expressed as mean ± SEM and come from 4 independent repetitions of 3 technical replicates. A star indicates a significant difference with the untreated cells ($P < 0.05$, Student's *t*-test with Bonferroni-Sidazk correction).

HO-1 expression due to AgNPs was measured in cells previously pre-incubated with ML-385 to investigate if Nrf2 pathway is involved. According to results of an LDH assay, this incubation with ML-385 was not toxic (Figure S3). The induction of HO-1 by AgNPs was counteracted when cells were pre-incubated with ML-385 in the presence of AgNPs, with a 4-fold decrease of HO-1 RNA levels (Fig. 11A). This tends to confirm that a concentration of 15 µg/mL AgNPs activates Nrf2 signalling pathway and that this effect was inhibited by ML-385. The pre-incubation with ML385 also significantly decreased the production of IL-8 mRNA by AgNPs, suggesting that Nrf2 could be a key to explain the mechanism of AgNPs induction of IL-8 (Fig 11B).

4. Discussion

With their increasing use in food-related consumer products, it is very likely that a certain proportion of these AgNPs are ingested and that they come in contact with IECs from the gut. Although the important role of these cells in immune regulation against luminal potential antigens has been well described, the effect of AgNPs on inflammation in IECs still remains largely unknown. This study analyses the implication of one of the key players of these mechanisms, *i.e.* IL-8 upon exposure of human intestinal Caco-2 cells to AgNPs and underlines the involvement of soluble Ag and Nrf2 signalling cascade in the secretion of IL-8. A preliminary characterisation of AgNPs was performed by TEM, DLS and spectrophotometry in the medium used for cell incubations and showed that nanoparticles were present in the material. After a 3 h incubation of differentiated Caco-2 cells with AgNPs followed by a recovery period, IL-8 levels increased time-dependently during this period, reaching a plateau after 21 h. IL-8 needs time to be synthesized within the cells and to be secreted. This also suggests that the protein of IL-8 is stable and not degraded during this duration. mRNA was extracted immediately after the incubation with AgNPs to avoid its degradation, because less time is required to produce mRNA than the translated protein. Indeed, IL-8 mRNA was already produced as soon as 45 min after the stimulus (Jijon et al., 2002), attaining a peak 2 h after the treatment (Yamamoto et al., 2003). Moreover, it was also shown that IL-8 mRNA was not stable and decreased after these 2 h (Lim et al., 2012). The recovery period for mRNA quantification was thus not relevant.

Our results indicated that AgNPs induced the IL-8 expression in Caco-2 cells as the quantity of the corresponding mRNA and related protein increased upon exposure to AgNPs. IL-8 levels were shown to decrease in the presence of AgNPs after 3 h incubation (Martirosyan et al., 2016). However, when cells have time to produce IL-8, this tendency is inverted and IL-8 is secreted in response to AgNPs stimulus as observed after the 21 h recovery period. Similar studies have also demonstrated the production of inflammatory cytokines in presence of AgNPs and, in particular, IL-8 both at the mRNA and at the protein level, on macrophages (Carlson et al., 2008; Kim and Choi, 2012; Orłowski et al., 2012; Lim et al., 2012; Martínez-Gutierrez et al., 2012),

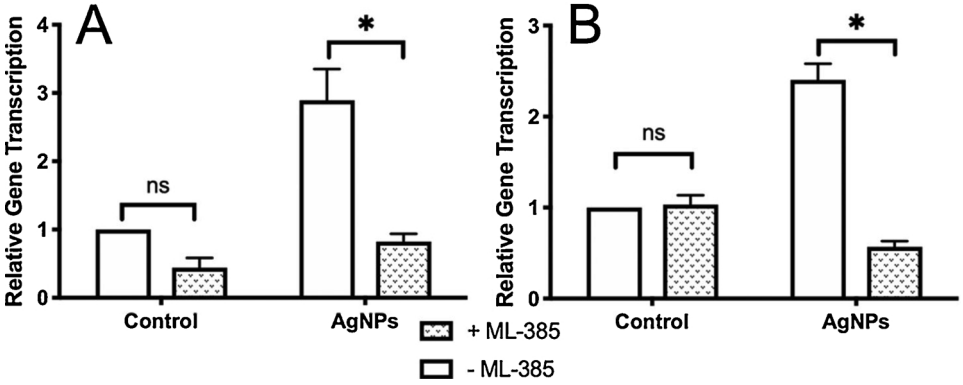

Fig. 11. Relative gene transcription of (A) HO-1 and (B) IL8 upon 3 h exposure of Caco-2 cells to 15 µg/mL AgNPs in cells preincubated or not during 24 h with ML-385 at 10 µM. Data are expressed as mean ± SEM and come from 4 independent repetitions of 3 technical replicates. A star indicates a significant difference caused by ML-385 while "ns" means non-significant difference ($P < 0.05$, Student's *t*-test with Bonferroni-Šidazk correction.

mesenchymal stem cells (Greulich et al., 2009; Jung et al., 2014; Hackenberg et al., 2011; Yang et al., 2012), peripheral blood mononuclear cells (Greulich et al., 2011; Yang et al., 2012), liver cells (Stępkowski et al., 2014) or keratinocytes (Samberg et al., 2009). This phenomenon occurs at subtoxic concentrations. Higher concentrations of AgNPs led to a cell mortality, decreasing the amount of secreted cytokines (Greulich et al., 2009). In our study, the highest tested concentration of 15 µg/mL was not cytotoxic (data not shown).

With regard to IECs lines, this induction of IL-8 has also been observed on Lovo cells (colonic cell line) with a AgNPs-size-dependent increase of IL-8 after 24 h incubation (Miethling-Graff et al., 2014). Similarly, an increase of IL-8 due to AgNPs was shown in Caco-2 cells (Georgantzopoulou et al., 2015; Chalew and Schwab, 2013; Gioria et al., 2018), which is in accordance with our observations on Caco-2 cells.

This IL-8 production by Caco-2 cells seems to be polarised towards the apical compartment, as basolateral level of IL-8 was only increased at the highest concentration of 15 µg/mL AgNPs. Apical secretion of IL-8 could appear surprising, as this chemokine is involved in the recruitment of subepithelial immune cells. However, this is consistent with other studies where the stimulus was applied apically (Fusunyan et al., 1998; Németh et al., 2007; Sonnier et al., 2010). Moreover, the presence of IL-8 has been observed *in vivo* in the colon of healthy volunteers suggesting the apical secretion of IL-8 by enterocytes (Keshavarzian et al., 1999). It was hypothesized that the polarised response of IECs could depend of the compartment stimulated (Sonnier et al., 2010). When TNF-α was added apically, IL-8 was secreted only in the apical compartment, contrary to a basolateral stimulation with TNF-α leading to a bilateral release of IL-8. This would also explain the basolateral secretion of IL-8 following incubation with the inflammatory cocktail that consists in cytokines applied basolateral and LPS in the apical compartment. Apically applied LPS has only a minor role in the secretion of IL-8 by Caco-2 (Schuerer-Maly et al., 1994; Sonnier et al., 2010; Van De Walle et al., 2010), contrarily to basolaterally applied cytokines (Van De Walle et al., 2010), which could polarise the secretion of IL-8 towards the basolateral compartment. In addition, it was discussed that the presence of IL-8 in the intestinal lumen could improve the chemotactic gradient of IL-8 and facilitate the transepithelial migration of neutrophils towards the inflammatory stimulus (Sonnier et al., 2010). Luminal IL-8 could also have a role in autocrine signalisation between IECs based on the presence of CXCR1, a receptor for IL-8, in the apical pole of Caco-2 cells, as well as in duodenal and colonic enterocytes (Rossi et al., 2013). In addition, the apical incubation of Caco-2 with IL-8 led to changes in the expression of genes involved in the regulation of cell differentiation and lipid metabolism, which suggests that apical IL-8 produced following AgNPs exposure could have a role in the communication between IECs (Rossi et al., 2013). IL-6, MCP-1 and IL-10 cytokine levels were also measured in our study but their levels remained below the detection limit. Similar results about an increase of IL-8 but not of other tested cytokines (IL-1β, IL-6 and TNFα) have been described after 2 h incubation of U937 human macrophages with 2.5 µg/mL AgNPs (Lim et al., 2012).

As AgNPs are known to oxidize and to form Ag^+, the involvement of these ions in the observed effects of AgNPs should be taken into account. In this study, we separated the soluble Ag fraction from AgNPs by centrifugal ultrafiltration, which allows to discriminate particles that stay on the filter from soluble Ag ions able to pass through. As filtrates do not present an absorbance peak around 410 nm such as AgNPs suspensions, it suggests that no particle was able to pass through the filter. This filtration was performed in water to avoid the formation of any precipitates. Indeed, because of the low solubility of silver salts, these Ag^+ could be present under other forms in the culture medium, with chloride salts precipitating at a higher rate than phosphate salts (Loza et al., 2014). Ultrafiltration followed by ICP-MS measurements is commonly used to quantify the amount of soluble Ag ions present in suspensions. After separation, soluble Ag passing through the filter can also be incubated with cells and compared with total AgNPs suspensions, containing AgNPs but also soluble Ag ions. Any additional effect when cells were treated with AgNPs suspensions would therefore originate from AgNPs. The release of IL-8 after incubation of cells with AgNPs suspensions was mainly mediated by the soluble fraction of silver in this suspension. Furthermore, a silver nitrate solution containing the same amount of Ag led to a similar secretion of IL-8. This is consistent with reports that the toxicity of AgNPs suspension on A549 cells, originating from a lung adenocarcinoma, was mainly mediated by the soluble Ag fraction (Beer et al., 2012). The uptake of AgNPs by Caco-2 cells has already been observed by some authors using TEM or confocal microscopy (Abdelkhaliq et al., 2019; Sahu et al., 2014; van der Zande et al., 2016; Vila et al., 2017). However, in this study, the internalised particles did not seem to affect IL-8 secretion, as the same amount of IL-8 was secreted in response to the soluble fraction of AgNPs. Some studies have also found that Ag^+ ions, in the form of silver nitrate, were able to induce the secretion of IL-8 by intestinal cells (Georgantzopoulou et al., 2015). The involvement of these ions could be a key to explain discrepancies between the different studies published about inflammatory properties of AgNPs. The importance of soluble Ag fraction relies on different parameters such as the synthesis method (Beer et al., 2012), the silver concentration (Hadioui et al., 2013), the size of AgNPs (Bouwmeester et al., 2011), their shape (Kent and Vikesland, 2012) or their coating (van der Zande et al., 2012).

NF-κB pathway is the main signalling cascade that regulates IL-8 secretion through the presence of element responses to NF-κB in IL-8 promoter (Hoffmann et al., 2002; Philpott et al., 2000). Indeed, the inflammatory cocktail, comprised of cytokines and LPS, well-known inducers of NF-κB, induced a large expression of IL-8. However, we have shown in a previous work that AgNPs were not able to activate the NF-κB signalling cascade, and even decreased its activation by the inflammatory cocktail (unpublished results). Other signalling cascades involved in the induction of IL-8 such as Nrf2 could also modulate the expression of this chemokine because the promoter of IL-8 also contains an ARE (Zhang et al., 2005).

As Nrf2 is induced as a response to oxidative stress in order to orchestrate cellular defences against oxidative stress, a NBT assay was used to show that AgNPs induced an oxidative stress, which is in agreement with other comparable studies performed on intestinal cells (Martirosyan et al., 2014, 2016, Böhmert et al., 2015; Gerloff et al., 2009). Moreover, different studies have observed a protective effect of a pre-treatment of cells with N-acetylcystein, a precursor of glutathione (Dodd et al., 2008) and a strong ROS scavenger, against AgNPs effects on cell viability (Chairuangkitti et al., 2013), DNA damages (Kang et al., 2012b), cell cycle (Chairuangkitti et al., 2013; Kang et al., 2012a), mitochondrial membrane potential (Chairuangkitti et al., 2013) or even glucose consumption (Lee et al., 2016). N-acetylcystein is also a silver ion chelator and this property could potentiate its protective effect on AgNPs toxicity. Similarly to N-acetylcystein, Nrf2 activation seems to alleviate deleterious effects of AgNPs. Indeed, Kang et al. (2012) have shown that the knockdown of Nrf2 cascade in cells increased dramatically their sensitivity to AgNPs (Kang et al., 2012b, a). To investigate the importance of this transduction cascade in the IL-8 secretion, a specific inhibitor of Nrf2, ML-385, which attaches to the DNA binding domain of Nrf2, avoiding its interaction with the promoter of target genes and therefore reducing its transcriptional activity (Singh et al., 2016) was used. The inhibition of Nrf2 with ML-385 led to a complete suppression of the HO-1 mRNA induction by AgNPs, as expected but also of IL-8, suggesting an involvement of Nrf2 in the AgNPs-induced IL-8 upregulation. It has been reported that an increased Nrf2 expression led to an increased expression of IL-8 at mRNA and protein level (Zhang et al., 2005). This is consistent with our observation that when Nrf2 is repressed (by the inhibitor ML-385), IL-8 transcription is blocked.

Different transcriptomic studies have indicated that Nrf2 was activated by AgNPs (Prasad et al., 2013; van der Zande et al., 2016; Mao

et al., 2018; Aueviriyavit et al., 2014; Ambrožová et al., 2017; Böhmert et al., 2015). In contrast, a few studies have observed a lower activation of Nrf2 in the presence of AgNPs (Piao et al., 2011; Lee et al., 2016). This inconsistency could be due to different physico-chemical properties of AgNPs but also a difference between cell lines (Simmons et al., 2011). For example, upon incubation with different metals, A549 cells were unable to induce Nrf2 to a high level in contrast with what was observed for HepG2 hepatocarcinoma cells. This could be explained by their high level of intracellular glutathione conferring an important antioxidative capacity. Moreover, they harbor a mutation in Keap 1, a major regulator of Nrf2 cascade (Böhmert et al., 2015; Simmons et al., 2011).

AgNPs activate the production of HO-1 as observed by the induction of its mRNA. HO-1 is commonly used as a target gene to assess the activation of Nrf2, because it has probably the best characterised ARE of any Nrf2 target gene (Simmons et al., 2011). HO-1 is also induced in liver cells (Stępkowski et al., 2014), HeLa cells (Miura and Shinohara, 2009), in macrophages (Lim et al., 2012), in an alveolar barrier model (Fizesan et al., 2019) and in Caco-2 cells (Böhmert et al., 2015), suggesting an activation of the Nrf2 cascade, as its expression is known to be dependent on the cellular redox status and Nrf2 signalling pathway (Keyse and Tyrrell, 1989; Alam et al., 1999). However, it can also be induced by other pathways such as AP-1 or NF-κB (Alam and Den, 1992; Lavrovsky et al., 1994). In our case, we have observed a complete inhibition of HO-1 production by the specific inhibitor of Nrf2, ML-385 suggesting that, in our experimental conditions, Nrf2 is necessary for HO-1 expression. Moreover, it seems that AgNPs induce HO-1 by a Nrf2 dependent pathway, as HO-1 induction by AgNPs does not occur in Nrf2 knockdown cells (Kang et al., 2012b). HO-1 protects cells from AgNPs toxicity, as the presence of a specific inhibitor decreases dramatically viability of cells while an activator of HO-1 protects them (Kang et al., 2012b). This Nrf2 pathway is activated to coordinate cellular responses to stress and seems to regulate the IL-8 secretion induced by AgNPs. Besides its pro-inflammatory properties, IL-8 could also have a protective role in enterocytes leading to the expression of genes involved in the regulation of cell differentiation and lipid metabolism, which could help to initiate responses against the potential loss of integrity due to chemicals (Rossi et al., 2013).

5. Conclusion

In summary, Caco-2 cells produce IL-8 in response to AgNPs exposure. This secretion is polarized towards the luminal compartment and is activated, at least partially, by a Nrf2 dependent pathway suggesting the involvement of oxidative stress in this secretion. This IL-8 secretion seems to be mediated by the soluble fraction composed of Ag^{+} ions present in AgNPs suspensions, suggesting that it is not specific to nanoparticles.

Funding information

The authors declare no conflict of interest. This work has received some financial support from Association Luxembourgeoise des Amis de la Fondation de l'Université Catholique de Louvain (ALAF) and from UCLouvain (FSR Grant).

Declaration of Competing Interest

The authors declare that they have no known competing financial interests or personal relationships that could have appeared to influence the work reported in this paper.

Acknowledgments

We would like to thank the SMCS platform from UCLouvain and in particular Vincent Bremhorst and Catherine Rasse for the statistical support.

Appendix A. Supplementary data

Supplementary material related to this article can be found, in the online version, at doi:https://doi.org/10.1016/j.toxlet.2020.02.004.

References

Abdelkhaliq, A., et al., 2019. Impact of in vitro digestion on gastrointestinal fate and uptake of silver nanoparticles with different surface modifications. Nanotoxicology 1–16.
Akter, M., et al., 2018. A systematic review on silver nanoparticles-induced cytotoxicity: physicochemical properties and perspectives. J. Adv. Res. 9, 1–16.
Alam, J., Den, Z., 1992. Distal AP-1 binding sites mediate basal level enhancement and TPA induction of the mouse heme oxygenase-1 gene. J. Biol. Chem. 267 (30), 21894–21900.
Alam, J., et al., 1999. Nrf2, a Cap'n'Collar transcription factor, regulates induction of the heme oxygenase-1 gene. J. Biol. Chem. 274 (37), 26071–26078.
Ambrožová, N., et al., 2017. Low concentrations of silver nanoparticles have a beneficial effect on wound healing *in vitro*. J. Nanopart. Res. 19 (3), 108.
Andoh, A., et al., 2000. Cytokine regulation of chemokine (IL-8, MCP-1, and RANTES) gene expression in human pancreatic periacinar myofibroblasts. Gastroenterology 119 (1), 211–219.
Artursson, P., 1990. Epithelial transport of drugs in cell culture. I: a model for studying the passive diffusion of drugs over intestinal absorbtive (Caco-2) cells. J. Pharm. Sci. 79 (6), 476–482.
Aueviriyavit, S., Phummiratch, D., Maniratanachote, R., 2014. Mechanistic study on the biological effects of silver and gold nanoparticles in Caco-2 cells–induction of the Nrf2/HO-1 pathway by high concentrations of silver nanoparticles. Toxicol. Lett. 224 (1), 73–83.
Beer, C., et al., 2012. Toxicity of silver nanoparticles nanoparticle or silver ion? Toxicol. Lett. 208 (3), 286–292 33.
Behra, R., et al., 2013. Bioavailability of silver nanoparticles and ions: from a chemical and biochemical perspective. J. R. Soc. Interface 10 (87) 20130396.
Bilberg, K., et al., 2011. Silver nanoparticles disrupt olfaction in Crucian carp (Carassius carassius) and Eurasian perch (Perca fluviatilis). Aquat. Toxicol. 104 (1-2), 145–152.
Blikslager, A.T., et al., 2007. Restoration of barrier function in injured intestinal mucosa. Physiol. Rev. 87 (2), 545–564.
Böhmert, L., et al., 2015. Molecular mechanism of silver nanoparticles in human intestinal cells. Nanotoxicology 9 (7), 852–860.
Bourlioux, P., et al., 2003. The intestine and its microflora are partners for the protection of the host: report on the Danone Symposium "the Intelligent Intestine," held in Paris, June 14, 2002. Am. J. Clin. Nutr. 78 (4), 675–683.
Bouwmeester, H., et al., 2011. Characterization of translocation of silver nanoparticles and effects on whole-genome gene expression using an *in vitro* intestinal epithelium coculture model. ACS Nano 5 (5), 4091–4103.
Braakhuis, H.M., et al., 2015. Progress and future of *in vitro* models to study translocation of nanoparticles. Arch. Toxicol. 89 (9), 1469–1495.
Carlson, C., et al., 2008. Unique cellular interaction of silver nanoparticles: size-dependent generation of reactive oxygen species. J. Phys. Chem. B 112 (43), 13608–13619.
Chairuangkitti, P., et al., 2013. Silver nanoparticles induce toxicity in A549 cells via ROS-dependent and ROS-independent pathways. Toxicol. Vitro 27 (1), 330–338.
Chalew, T.E.A., Schwab, K.J., 2013. Toxicity of commercially available engineered nanoparticles to Caco-2 and SW480 human intestinal epithelial cells. Cell Biol. Toxicol. 29 (2), 101–116.
Cushen, M., et al., 2014. Evaluation and simulation of silver and copper nanoparticle migration from polyethylene nanocomposites to food and an associated exposure assessment. J. Agric. Food Chem. 62 (6), 1403–1411.
Dodd, S., et al., 2008. N-acetylcysteine for antioxidant therapy: pharmacology and clinical utility. Expert Opin. Biol. Ther. 8 (12), 1955–1962.
Echegoyen, Y., Nerín, C., 2013. Nanoparticle release from nano-silver antimicrobial food containers. Food Chem. Toxicol. 62, 16–22.
Eckmann, L., et al., 1995. Entamoeba histolytica trophozoites induce an inflammatory cytokine response by cultured human cells through the paracrine action of cytolytically released interleukin-1 alpha. J. Clin. Investig. 96 (3), 1269–1279.
El-Nour, K.M.A., et al., 2010. Synthesis and applications of silver nanoparticles. Arab. J. Chem. 3 (3), 135–140.
Emamifar, A., et al., 2012. Effect of nanocomposite packaging containing Ag and ZnO on reducing pasteurization temperature of orange juice. J. Food Process. Preserv. 36 (2), 104–112.
Fizesan, I., et al., 2019. In vitro exposure of a 3d-tetraculture representative for the alveolar barrier at the air-liquid interface to silver particles and nanowires. Part. Fibre Toxicol. 16 (1), 14.
Fogh, J., Trempe, G., 1975. New human tumor cell lines. Human Tumor Cells in Vitro. Springer, pp. 115–159.
Fusunyan, R.D., et al., 1998. Butyrate enhances interleukin (IL)-8 secretion by intestinal epithelial cells in response to IL-1β and lipopolysaccharide. Pediatr. Res. 43 (1), 84.
Gaillet, S., Rouanet, J.M., 2015. Silver nanoparticles: their potential toxic effects after oral exposure and underlying mechanisms–a review. Food Chem. Toxicol. 77, 58–63.
Georgantzopoulou, A., et al., 2015. Effects of silver nanoparticles and ions on a co-culture model for the gastrointestinal epithelium. Part. Fibre Toxicol. 13 (1), 9.
Gerloff, K., et al., 2009. Cytotoxicity and oxidative DNA damage by nanoparticles in

human intestinal Caco-2 cells. Nanotoxicology 3 (4), 355–364.
Gioria, S., et al., 2018. Proteomics study of silver nanoparticles on Caco-2 cells. Toxicol. Vitr. 50, 347–372.
Gozzelino, R., Jeney, V., Soares, M.P., 2010. Mechanisms of cell protection by heme oxygenase-1. Annu. Rev. Pharmacol. Toxicol. 50, 323–354.
Greulich, C., et al., 2009. Studies on the biocompatibility and the interaction of silver nanoparticles with human mesenchymal stem cells (hMSCs). Langenbecks Arch. Surg. 394 (3), 495–502.
Greulich, C., et al., 2011. Uptake and intracellular distribution of silver nanoparticles in human mesenchymal stem cells. Acta Biomater. 7 (1), 347–354.
Hackenberg, S., et al., 2011. Silver nanoparticles: evaluation of DNA damage, toxicity and functional impairment in human mesenchymal stem cells. Toxicol. Lett. 201 (1), 27–33.
Hadioui, M., Leclerc, S., Wilkinson, K.J., 2013. Multimethod quantification of Ag+ release from nanosilver. Talanta 105, 15–19.
Hauri, J.F., Niece, B.K., 2011. Leaching of silver from silver-impregnated food storage containers. J. Chem. Educ. 88 (10), 1407–1409.
Hoffmann, E., et al., 2002. Multiple control of interleukin-8 gene expression. J. Leukoc. Biol. 72 (5), 847–855.
Hollebeeck, S., et al., 2012. Anti-inflammatory effects of pomegranate (Punica granatum L.) husk ellagitannins in Caco-2 cells, an *in vitro* model of human intestine. Food Funct. 3 (8), 875–885.
Jijon, H.B., et al., 2002. MAP kinases contribute to IL-8 secretion by intestinal epithelial cells via a post-transcriptional mechanism. Am. J. Physiol. Cell Physiol.
Jung, H.J., et al., 2014. Silver wire amplifies the signaling mechanism for IL1beta production more than silver submicroparticles in human monocytic THP-1 cells. PLoS One 9 (11), e112256.
Kang, S.J., et al., 2012a. Silver nanoparticles-mediated G2/M cycle arrest of renal epithelial cells is associated with Nrf2-GSH signaling. Toxicol. Lett. 211 (3), 334–341.
Kang, S.J., et al., 2012b. Role of the Nrf2-heme oxygenase-1 pathway in silver nanoparticle-mediated cytotoxicity. Toxicol. Appl. Pharmacol. 258 (1), 89–98.
Kaulmann, A., et al., 2016. Inflammation related responses of intestinal cells to plum and cabbage digesta with differential carotenoid and polyphenol profiles following simulated gastrointestinal digestion. Mol. Nutr. Food Res. 60 (5), 992–1005.
Kensler, T.W., Wakabayashi, N., Biswal, S., 2007. Cell survival responses to environmental stresses via the Keap1-Nrf2-ARE pathway. Annu. Rev. Pharmacol. Toxicol. 47, 89–116.
Kent, R.D., Vikesland, P.J., 2012. Controlled evaluation of silver nanoparticle dissolution using atomic force microscopy. Environ. Sci. Technol. 46 (13), 6977–6984.
Keshavarzian, A., et al., 1999. Leaky gut in alcoholic cirrhosis: a possible mechanism for alcohol-induced liver damage. Am. J. Gastroenterol. 94 (1), 200.
Keyse, S.M., Tyrrell, R.M., 1989. Heme oxygenase is the major 32-kDa stress protein induced in human skin fibroblasts by UVA radiation, hydrogen peroxide, and sodium arsenite. Proc. Natl. Acad. Sci. 86 (1), 99–103.
Kim, S., Choi, I.H., 2012. Phagocytosis and endocytosis of silver nanoparticles induce interleukin-8 production in human macrophages. Yonsei Med. J. 53 (3), 654–657.
Klein, C., et al., 2011. NM-series of representative manufactured nanomaterials: NM-300 silver characterisation, stability, homogeneity. Jrc Scientific and Technical Reports. available at. https://core.ac.uk/download/pdf/38621213.pdf.
Klein, S.G., et al., 2017. Endothelial responses of the alveolar barrier *in vitro* in a dose-controlled exposure to diesel exhaust particulate matter. Part. Fibre Toxicol. 14 (1), 7.
Kobayashi, M., Yamamoto, M., 2005. Molecular mechanisms activating the Nrf2-Keap1 pathway of antioxidant gene regulation. Antioxid. Redox Signal. 7 (3-4), 385–394.
Kwak, M.K., Wakabayashi, N., Kensler, T.W., 2004. Chemoprevention through the Keap1-Nrf2 signaling pathway by phase 2 enzyme inducers. Mutat. Res. Mol. Mech. Mutagen. 555 (1-2), 133–148.
Laloux, L., Polet, M., Schneider, Y.J., 2017. Interaction between ingestedengineered nanomaterials and the gastrointestinal tract: in vitro toxicology aspects. Nanotechnol. Agric. Food Sci.
Larsen, P., et al., 2015. Exposure assessment of nanomaterials in consumer products. Danish Environmental Protection Agency Environmental Project. pp. 1636.
Lavrovsky, Y., et al., 1994. Identification of binding sites for transcription factors NF-kappa B and AP-2 in the promoter region of the human heme oxygenase 1 gene. Proc. Natl. Acad. Sci. 91 (13), 5987–5991.
Lee, M.J., et al., 2016. Silver nanoparticles affect glucose metabolism in hepatoma cells through production of reactive oxygen species. Int. J. Nanomed. 11, 55.
León-Silva, S., Fernández-Luqueño, F., López-Valdez, F., 2016. Silver nanoparticles (AgNP) in the environment: a review of potential risks on human and environmental health. Water Air Soil Pollut. 227 (306), 1–20.
Lim, D.H., et al., 2012. The effects of sub-lethal concentrations of silver nanoparticles on inflammatory and stress genes in human macrophages using cDNA microarray analysis. Biomaterials 33 (18), 4690–4699.
Livak, K.J., Schmittgen, T.D., 2001. Analysis of relative gene expression data using real-time quantitative PCR and the 2ΔΔCt method. methods 25 (4), 402–408.
Loza, K., et al., 2014. The predominant species of ionic silver in biological media is colloidally dispersed nanoparticulate silver chloride. RSC Adv. 4 (67), 35290–35297.
Mao, B.H., et al., 2018. Silver nanoparticles have lethal and sublethal adverse effects on development and longevity by inducing ROS-mediated stress responses. Sci. Rep. 8 (1), 2445.
Martínez-Gutierrez, F., et al., 2012. Antibacterial activity, inflammatory response, coagulation and cytotoxicity effects of silver nanoparticles. Nanomed. Nanotechnol. Biol. Med. 8 (3), 328–336.
Martirosyan, A., Bazes, A., Schneider, Y.J., 2014. In vitro toxicity assessment of silver nanoparticles in the presence of phenolic compounds– preventive agents against the harmful effect? Nanotoxicology 8 (5), 573–582.
Martirosyan, A., et al., 2016. Tuning the inflammatory response to silver nanoparticles via quercetin in Caco-2 (co-) cultures as model of the human intestinal mucosa. Toxicol. Lett. 253, 36–45.
Mason, K.L., et al., 2008. Overview of Gut Immunology. Gi Microbiota and Regulation of the Immune System. Springer, pp. 1–14.
Miethling-Graff, R., et al., 2014. Exposure to silver nanoparticles induces sizeand dose-dependent oxidative stress and cytotoxicity in human colon carcinoma cells. Toxicol. Vitro 28 (7), 1280–1289.
Miura, N., Shinohara, Y., 2009. Cytotoxic effect and apoptosis induction by silver nanoparticles in HeLa cells. Biochem. Biophys. Res. Commun. 390 (3), 733–737.
Navarro, E., et al., 2008. Toxicity of silver nanoparticles to Chlamydomonas reinhardtii. Environ. Sci. Technol. 42 (23), 8959–8964.
Németh, E., et al., 2007. Effect of hydrogen peroxide on interleukin-8 synthesis and death of Caco-2 cells. Immunopharmacol. Immunotoxicol. 29 (2), 297–310.
Orłowski, P., et al., 2012. Toxicity of silver nanoparticles in monocytes and keratinocytes: potential to induce inflammatory reactions. Centr eur j immunol 37, 123–130.
Philpott, D.J., et al., 2000. Invasive Shigella flexneri activates NF-κB through a lipopolysaccharide-dependent innate intracellular response and leads to IL-8 expression in epithelial cells. J. Immunol. 165 (2), 903–914.
Piao, M.J., et al., 2011. Silver nanoparticles induce oxidative cell damage in human liver cells through inhibition of reduced glutathione and induction of mitochondria-involved apoptosis. Toxicol. Lett. 201 (1), 92–100.
Prasad, R.Y., et al., 2013. Investigating oxidative stress and inflammatory responses elicited by silver nanoparticles using high-throughput reporter genes in HepG2 cells: effect of size, surface coating, and intracellular uptake. Toxicol. Vitro 27 (6).
Reidy, B., et al., 2013. Mechanisms of silver nanoparticle release, transformation and toxicity: a critical review of current knowledge and recommendations for future studies and applications. Materials 6 (6), 2295–2350.
Rossi, O., et al., 2013. Vectorial secretion of interleukin-8 mediates autocrine signalling in intestinal epithelial cells via apically located CXCR1. BMC Res. Notes 6 (1), 431.
Ryter, S.W., Alam, J., Choi, A.M., 2006. Heme oxygenase-1/carbon monoxide: from basic science to therapeutic applications. Physiol. Rev. 86 (2), 583–650.
Sahu, S.C., et al., 2014. Comparative cytotoxicity of nanosilver in human liver HepG2 and colon Caco2 cells in culture. J. Appl. Toxicol. 34 (11), 1155–1166.
Sahu, B.D., et al., 2015. Lagerstroemia speciosa L. attenuates apoptosis in isoproterenol-induced cardiotoxic mice by inhibiting oxidative stress: possible role of Nrf2/HO-1. Cardiovasc. Toxicol. 15 (1), 10–22.
Salminen, S., et al., 1998. Functional food science and gastrointestinal physiology and function. Br. J. Nutr. 80 (S1), S147–S171.
Samberg, M.E., Oldenburg, S.J., Monteiro-Riviere, N.A., 2009. Evaluation of silver nanoparticle toxicity in skin in vivo and keratinocytes in vitro. Environ. Health Perspect. 118 (3), 407–413.
Sambuy, Y., et al., 2005. The Caco-2 cell line as a model of the intestinal barrier: influence of cell and culture-related factors on Caco-2 cell functional characteristics. Cell Biol. Toxicol. 21 (1), 1–26.
Schuerer-Maly, C., et al., 1994. Colonic epithelial cell lines as a source of interleukin-8: stimulation by inflammatory cytokines and bacterial lipopolysaccharide. Immunology 81 (1), 85.
Sergent, T., et al., 2010. Anti-inflammatory effects of dietary phenolic compounds in an *in vitro* model of inflamed human intestinal epithelium. Chem. Biol. Interact. 188 (3), 659–667.
Šidák, Z., 1967. Rectangular confidence regions for the means of multivariate normal distributions. J. Am. Stat. Assoc. 62 (318), 626–633.
Simmons, S.O., et al., 2011. Nrf2 oxidative stress induced by heavy metals is cell type dependent. Curr. Chem. Genomics 5, 1.
Singh, A., et al., 2016. Small molecule inhibitor of Nrf2 selectively intervenes therapeutic resistance in Keap1-deficient NSCLC tumors. ACS Chem. Biol. 11 (11), 3214–3225.
Smetanová, L., et al., 2011. Caco-2 cells, biopharmaceutics classification system (BCS) and biowaiver. Acta medica (hradec kralove) 54 (1), 3–8.
Song, H., et al., 2011. Migration of silver from nanosilver–polyethylene composite packaging into food simulants. Food Addit. Contam. Part A 28 (12), 1758–1762.
Sonnier, D.I., et al., 2010. TNF-α induces vectorial secretion of IL-8 in Caco-2 cells. J. Gastrointest. Surg. 14 (10), 1592–1599.
Stępkowski, T., Brzóska, K., Kruszewski, M., 2014. Silver nanoparticles induced changes in the expression of NF-κB related genes are cell type specific and related to the basal activity of NF-κB. Toxicol. Vitr. 28 (4), 473–478.
Syafiuddin, A., et al., 2017. A review of silver nanoparticles: research trends, global consumption, synthesis, properties, and future challenges. J. Chinese Chem. Soc. 64 (7), 732–756.
The project on emerging nanotechnologies, 2019. Consumer Products Inventory. http://www.nanotechproject.org/cpi.
Van De Walle, J., et al., 2010. Inflammatory parameters in Caco-2 cells: effect of stimuli nature, concentration, combination and cell differentiation. Toxicol. Vitro 24 (5), 1441–1449.
van der Zande, M., et al., 2012. Distribution, elimination, and toxicity of silver nanoparticles and silver ions in rats after 28-day oral exposure. ACS Nano 6 (8), 7427–7442.
van der Zande, M., et al., 2016. Different responses of Caco-2 and MCF-7 cells to silver nanoparticles are based on highly similar mechanisms of action. Nanotoxicology 10 (10), 1431–1441.
Verleysen, E., et al., 2015. TEM and SP-ICP-MS analysis of the release of silver nanoparticles from decoration of pastry. J. Agric. Food Chem. 63 (13), 3570–3578.
Vigneshwaran, N., et al., 2007. Functional finishing of cotton fabrics using silver nanoparticles. J. Nanosci. Nanotechnol. 7 (6), 1893–1897.
Vila, L., Marcos, R., Hernández, A., 2017. Long-term effects of silver nanoparticles in caco-2 cells. Nanotoxicology 11 (6), 771–780.

Völker, C., et al., 2013. Comparative toxicity assessment of nanosilver on three Daphnia species in acute, chronic and multi-generation experiments. PLoS One 8 (10), e75026.
von Goetz, N., et al., 2013. Migration of silver from commercial plastic food containers and implications for consumer exposure assessment. Food Addit. Contam. Part A 30 (3), 612–620.
Wang, X., Seed, B., 2003. PrimerBank: a resource of human and mouse PCR primer pairs for gene expression detection and quantification. Nucleic Acids Res. 31 (24), 1–8.
Wijnhoven, S.W., et al., 2009. Nano-silver–a review of available data and knowledge gaps in human and environmental risk assessment. Nanotoxicology 3 (2), 109–138.
Xin, L., et al., 2015. Increased oxidative stress and activated heat shock proteins in human cell lines by silver nanoparticles. Hum. Exp. Toxicol. 34 (3), 315–323.
Yamamoto, K., et al., 2003. Combined effect of hydrogen peroxide induced oxidative stress and IL-1α on IL-8 production in Caco-2 cells (a human colon carcinoma cell line) and normal intestinal epithelial cells. Inflammation 27 (3), 123–128.
Yang, E.J., et al., 2012. Inflammasome formation and IL-1β release by human blood monocytes in response to silver nanoparticles. Biomaterials 33 (28), 6858–6867.
Yin, L., et al., 2011. More than the ions: the effects of silver nanoparticles on Lolium multiflorum. Environ. Sci. Technol. 45 (6), 2360–2367.
Zhang, X., et al., 2005. Activation of the Nrf2/antioxidant response pathway increases IL-8 expression. Eur. J. Immunol. 35 (11), 3258–3267.
Zhao, C.M., Wang, W.X., 2012. Importance of surface coatings and soluble silver in silver nanoparticles toxicity to Daphnia magna. Nanotoxicology 6 (4), 361–370.
Zhu, X., et al., 2011. Heme oxygenase-1 system and gastrointestinal inflammation: a short review. World J. Gastroenterol.: Wjg 17 (38), 4283.